16th World Conference on Earthquake, 16WCEE 2017

Santiago Chile, January 9th to 13th 2017

Paper N° 4359 (Abstract ID)

Registration Code: S-K1464748820

Performance of Fire Sprinkler Systems in the 2014 South Napa Earthquake: Computational Modeling with Validation by Laser Scans

S. Takhirov[1], K.M. Mosalam[2], F. Cakir [3], S. Günay[4]

[1] Structures Laboratory Manager, University of California, Berkeley, takhirov@berkeley.edu
[2] Taisei Professor of Civil Engineering and PEER Director, University of California, Berkeley, mosalam@berkeley.edu
[3] Visiting Scholar, Pacific Earthquake Engineering Research Center, University of California, Berkeley, feritcakir@berkeley.edu
[4] Project Scientist, University of California, Berkeley, selimgunay@berkeley.edu

Abstract

Several failures of fire sprinkler systems were observed after the 2014 South Napa earthquake, California, USA. In many cases, the failures were related to excessive displacements of these systems that led to interaction with the surrounding nonstructural components, e.g. suspended ceiling systems, light fixtures, and ventilation ducts. Due to this interaction and associated impact loading during the earthquake, some failures in pipe joints and sprinkler systems were observed. Since the fire hazard following the earthquake was still present right after the earthquake, the valves supplying water to the fire protection system were not closed for hours. As a result, water flooding damage of the contents of buildings occurred. Although such damage was relatively minor in some of the buildings, failure of the fire sprinkler system in a department store caused closure of the store for more than nine months and the store was eventually transferred to a new location. The total monetary loss associated with the goods damaged by water, lost wages and lost revenue can be in the order of hundreds of millions. In another case, the County Office Building, a two-story concrete shear wall structure, was subject to significant water damage due to sprinkler head failure upon potential impact with other nonstructural components. The sprinkler system ran for five hours without being shut off. All partition walls and floor coverings sustained extensive water damage, leading to the closure of the building for months. To investigate this significant performance problem introduced by such nonstructural components, the research team conducted laser scans of a parking structure with an exposed fire sprinkler system, which encountered a number of failures with some residual deformation. All these anomalies were captured by a laser scanner. An accurate computational model of the building and the fire sprinkler system was developed using the scanned geometry and the finite element method. Linear time history analyses were conducted on this detailed finite element model using the three components of a ground motion recorded near the building. The analysis results were compatible with the damage observed in the piping system.

Keywords: finite element method; fire sprinkler systems; laser scanning; nonstructural components; seismic performance; time history analysis.

1. Introduction

The August 24, 2014 South Napa earthquake occurred on the West Napa fault, which is within a 70 km (44 miles) wide set of faults that constitutes the San Andreas fault system. With a moment magnitude of 6.0, the event was the largest in the San Francisco Bay Area since the 1989 Loma Prieta earthquake. It was a moderate earthquake that revealed relatively limited structural performance issues. Nevertheless, there was quite significant monetary losses due to poor performance of nonstructural components. Field observations and detailed analysis of the earthquake aftermath were summarized in many publications [e.g. 1, 2]. Among 68 buildings studied in FEMA P1024 [1], damage to contents was the most common, with 24% experiencing a significant level of loss. Damage to lights and ceilings was the next most common that was observed in 16% of the buildings. A total of 32 buildings (47%) investigated in [1] had fire sprinkler systems where damage was reported in five buildings. It was reported that in one case of a parking structure with exposed fire-fighting piping system, the damage was very minor and was limited to a number of short pipe hangers failed in an unbraced sprinkler system without water leakage. On the other hand, the sprinkler system experienced leakage in another building, causing damage to an ornamental plaster ceiling. The most severe failures of sprinkler systems were observed in three of the five buildings investigated in [1] that resulted in flooding and significant damage to floor coverings and partitions. In addition to the failures analyzed in [1], the authors witnessed a number of similar failures of fire sprinkler systems in other buildings [2].

Failures of the fire sprinkler system lead to distinguishably different consequences than those of other nonstructural components and systems. A failure in a sprinkler system has a high potential of cascading effect because water propagates through several levels of a building by affecting everything on its way. The flooding can cause complete collapse of suspended ceiling system (including the light fixtures) under increased weight of soaked lay-in panels. Furthermore, it can damage the interior of a building including flooring and partitions and destroy the contents of the building that, in some cases, are more expensive than the building itself. Therefore, a failure in a fire sprinkler system can result in an inhabitable building with totaled content that leads to a long downtime and significant monetary losses.

2. Example of Department Store

A department store building that experienced failure of its fire sprinkler system [1, 2] is discussed in this section to show consequences of the poor performance of the piping system. The store was a two-story building of mixed construction. The roof was built with plywood supported by wood framing, glulam beams, and steel columns. The second floor included gypsum concrete fill on plywood supported by manufactured trusses, glulam beams, and steel columns. The lateral load supporting system included pre-Northridge moment frames, chevron-braced frames, and plywood shear walls. A tenant introduced some improvements in 1987. The date of building construction was not known but it was estimated as mid-1980s. Water was released from five lines suspended from the roof for at least six hours (Fig. 1). The elevator and escalator pits were flooded, and both systems required repair. Building content was damaged as a result of water and soaked lay-in panels dropped on it (Fig. 2) and some merchandise racks were overturned. Considerable amounts of gypsum wallboards were water damaged and required removal. The suspended acoustic tile ceiling was severely damaged, including damage to its grid. Due to increased weight of the system “free” ends came off wall moldings, “fixed” ends pulled out of the wall moldings, and splices failed. It is noted that partitions were braced by the ceilings and may have contributed to the ceiling damage at some locations.

Photograph of store while water flooding was taking place

Photograph of store after water was turned off (pressure of a water head punched a hole in the parapet)

Fig. 1 – External observations of fire sprinkler system failure in the two-story retail store

The store was closed during the earthquake (the event occurred at 3:20 am) and remained closed after the event. When its condition was checked after 9 months, it was still closed. The tenant was faced with major repairs, that, in addition to repair of the fire sprinkler systems and replacement of suspended ceiling systems, included replacement of all plaster boards, electrical, heating and cooling systems, repair of elevator and escalator systems, and removal of mold that had taken over the building due to the flooding. Such extensive repairs would have triggered bringing the store up to current building codes, adding yet another layer of expense. As a result, the tenant decided to stop its operations at this location that was announced eleven months after the earthquake [3]. Moreover, these repair expenses were in excess of other losses: (1) value of the store's merchandize and other valuable content right before the earthquake, (2) lost revenue and lost wages for employees, and (3) lost sales. As shown in Fig. 3, the latter losses could be close to 92% (11 months of non-operation out of 12 months) of $98.1 million for a leading department store [4] and of $137.2 million for a leading retail store [4].

Soaked and partially dissolved lay-in panels on the floor and merchandise

Flooded floor with merchandise on the floor

Fig. 2 – Visual observations of the first floor content damage due to water leakage from the second floor

If the tenant would be a leading US department store it could lose 92% of $98.1M in sales (source – Statista)

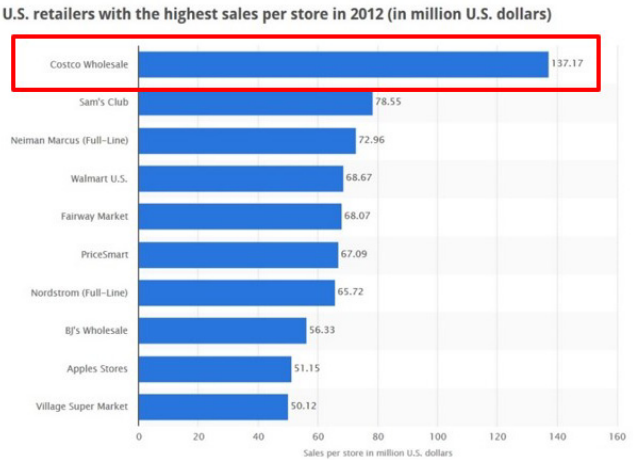

If the tenant would be a leading US retail store it could lose 92% of $137.2M in sales (source – Statista)

Fig. 3 – Possible scenarios in lost sales for two hypothetical tenants

3. Piping System in a Parking Structure: Laser Scans

The building discussed above had very limited accessibility after the earthquake due to severe damage and legal issues associated with the cost of the content, repairs, and replacements. Therefore, it was not examined further by the authors. A parking structure in the immediate vicinity of the department store that had an exposed fire sprinkler system was investigated instead. Although no water leakage occurred, multiple failures of short pipe hangers were observed in an unbraced sprinkler system [2]. In addition to the conventional photographs, the failures were documented by a terrestrial laser scanner.

The damaged condition of the piping system on the third floor of the parking structure was scanned from thirteen stations. A terrestrial laser scanner, namely Scan Station C10 from Leica Geosystems, was utilized. The point clouds were stitched in the Cyclone application [5] and the final point cloud is presented in Fig. 4a.

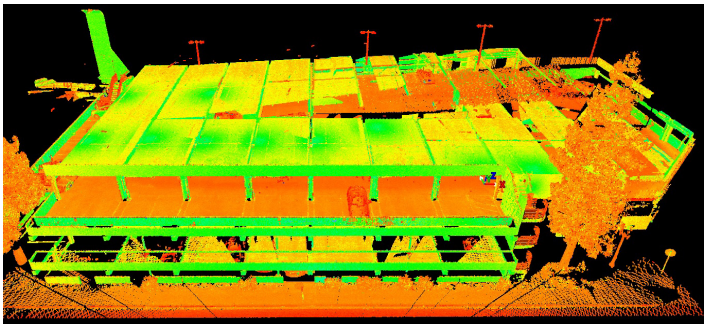

a) Global view

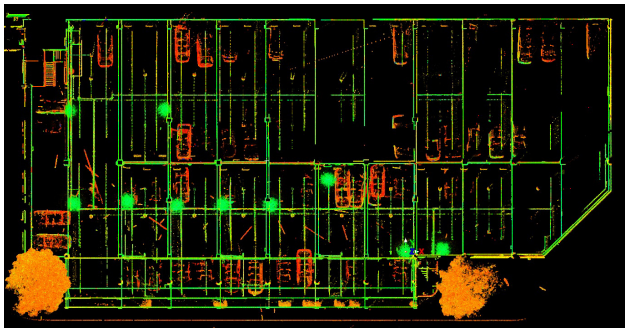

b) Plan view

Fig. 4 – Stitched point clouds of the parking structure and damaged fire sprinkler system

A plan view of the point cloud showing details of the piping system in presented in Fig. 4b. A zoomed in portion of the point cloud is shown in Fig. 5. The point cloud is colored based on real colors of the system captured by a still imaging camera built into the scanner. It shows residual displacements of the piping system that can be clearly estimated by the exposed amount of unpainted part of the pipes that used to be hidden by bracket of a hanger rod. The superposed ellipses show the bracket locations and the double headed arrows show directivity of the motion. All details of the piping system were captured and documented by the laser scanner including: (1) location of each pipe in space including residual deformations, if any, (2) the diameter of the pipe, (3) the location of the hanger rod in space, (4) the diameter and length of the rod, (5) the residual displacements along the longitudinal axis of the pipe, … etc. Some of the examples of subsequent measurements from the point cloud

are provided in Fig. 6. Two major failure modes were identified as presented in Fig. 7. The first mode (Fig. 7a) is most likely related to ultra-low cycle fatigue in the hanger rod that is subjected to limited number of large cycles. The second type of failure (Fig. 7b) is most likely related to excessive pull-out load and/or under-designed depth of the installed anchors. All failure locations were accurately captured by the laser scanner.

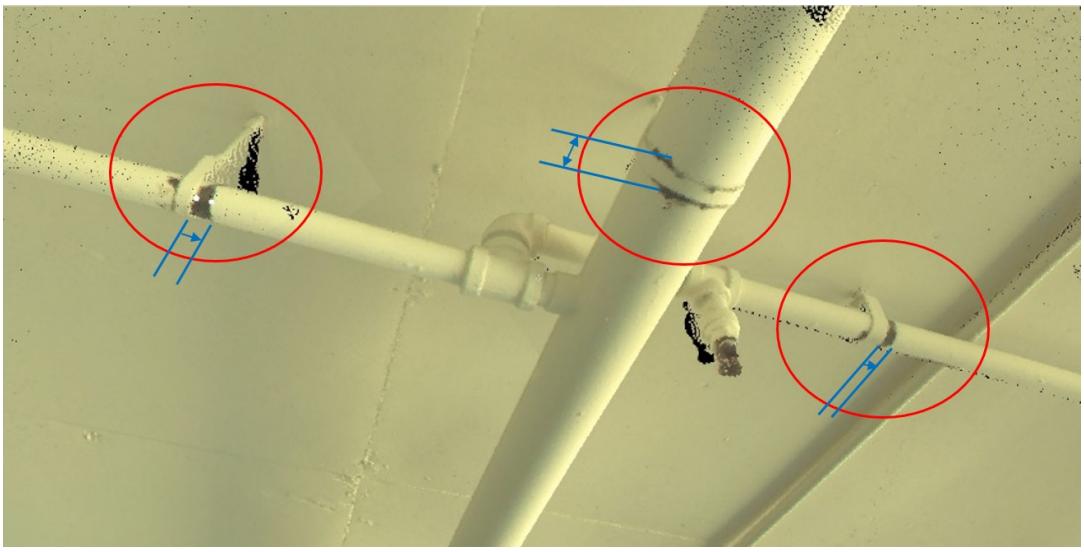

Fig. 5 – Zoomed view of the point cloud (colored by photo images)

The point cloud was used to model the building and the piping system itself as presented in Fig. 8. The Cyclone application [5] was used to convert the point cloud into solids. A zoomed view of the model of the building integrated with fire sprinkler system is presented in Figs. 8 and 9. This solid model was imported into ANSYS [6] to generate the finite element models of both the building and the piping system.

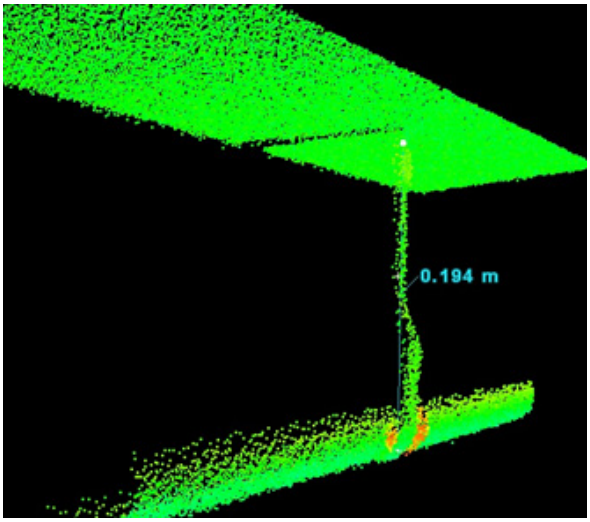

Length of hanger rod

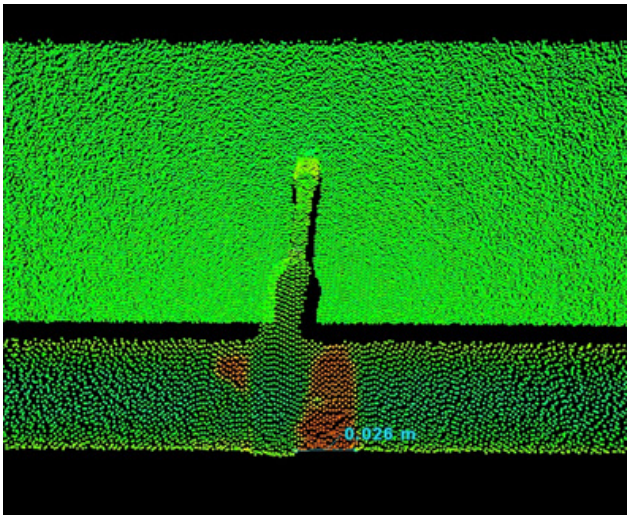

Residual displacement based on exposed unpainted surface and paint scratches

Fig. 6 – Sample local measurements from the point cloud

Residual deformations of the piping system were distributed throughout the system. The deformation was quantified by separating the point cloud of each individual pipe and examining its shape in space. Matlab [7] was used to slice the point cloud of the pipe in the transversal direction and to best fit the section to a circle. The center of the circle was assumed to be located on the axis of the deformed pipe at the cross section of the pipe. The slices were repeated at multiple locations with pre-defined periodicity of 1.5 times the pipe's diameter.A

typical result for the main pipe right next to its connection to one of the walls of the structure is presented in Fig. 10. The results are amplified by a factor of 100 to make the residual deflection of the pipe visible.

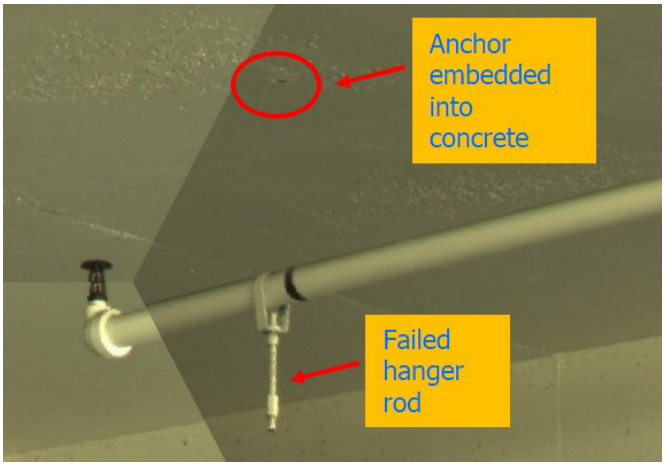

Failure of hanger rod at anchor

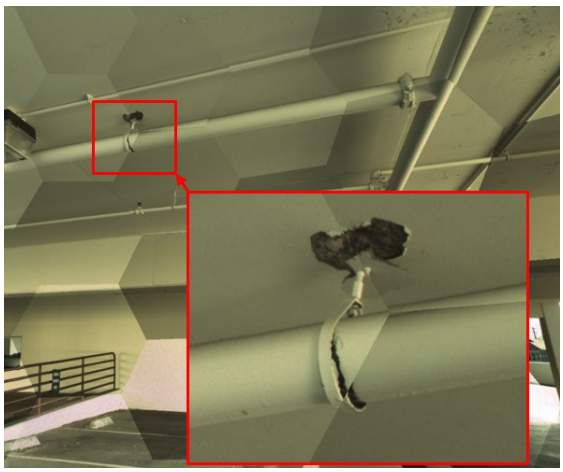

Hanger rod and its anchor pulled-out from concrete floor

Fig. 7 – Typical failure modes captured by laser scanner

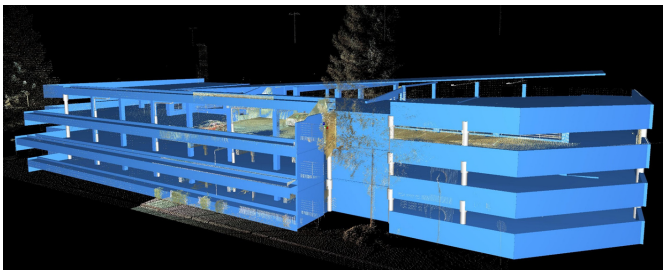

a) Structure

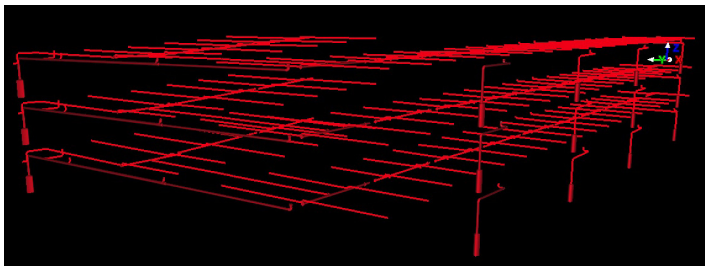

b) Piping system

Fig. 8 – Model of the structure and piping system

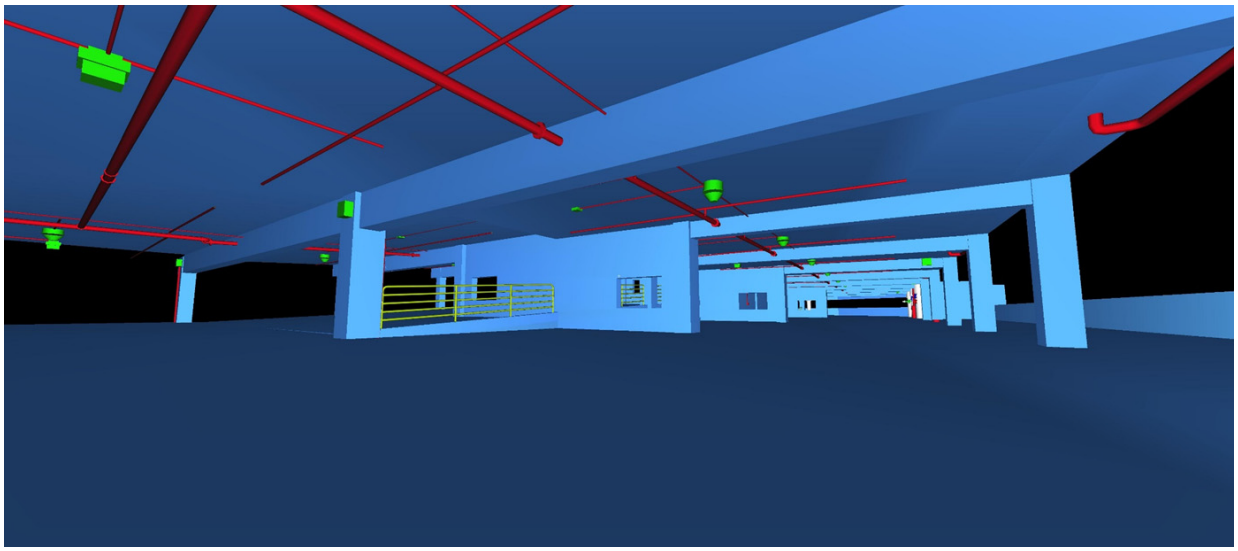

Fig. 9 – Integrated model of the buildings (blue) and the piping system (red).

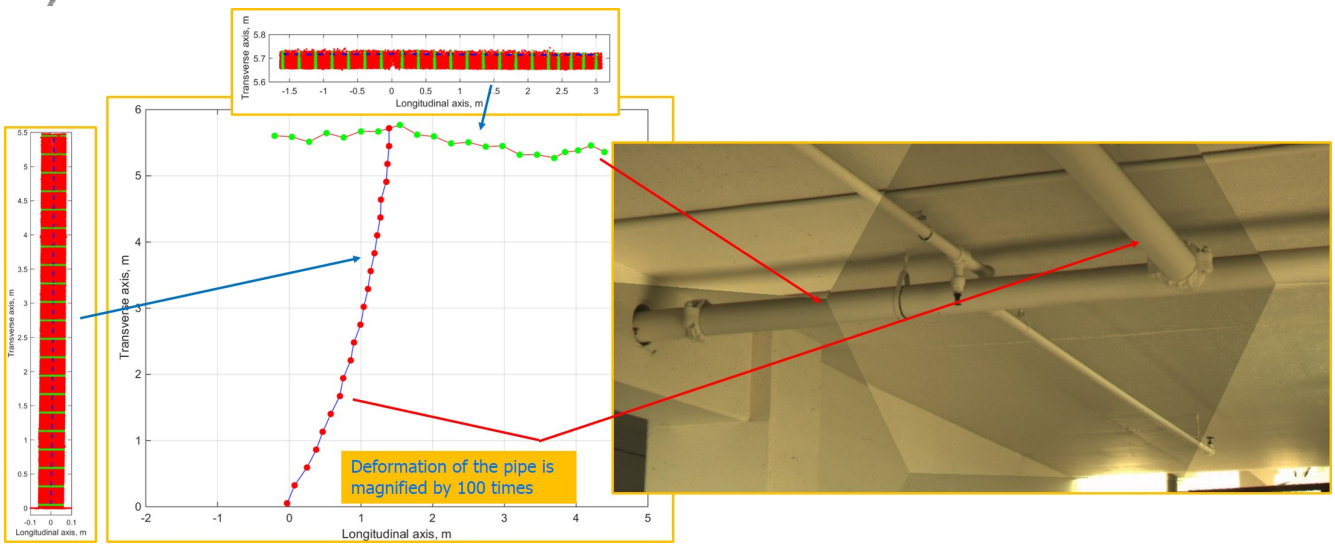

Fig. 10 – Residual deformation of the pipe estimated from the point cloud

4. Seismic Excitation Recorded in Vicinity of the Parking Structure

Station N016 from the USGS-NCSN strong motion network is within 500 meters from the parking structure as presented in the left part of Fig. 11. Because the accelerations recorded in this station are along the North-South and East-West directions, they were transformed to the accelerations along the two orthogonal directions (x and y) of the building as shown in the right part of Fig. 11. The transformed accelerations are plotted in Fig. 12, while the response spectra of these accelerations are plotted in Fig. 13.

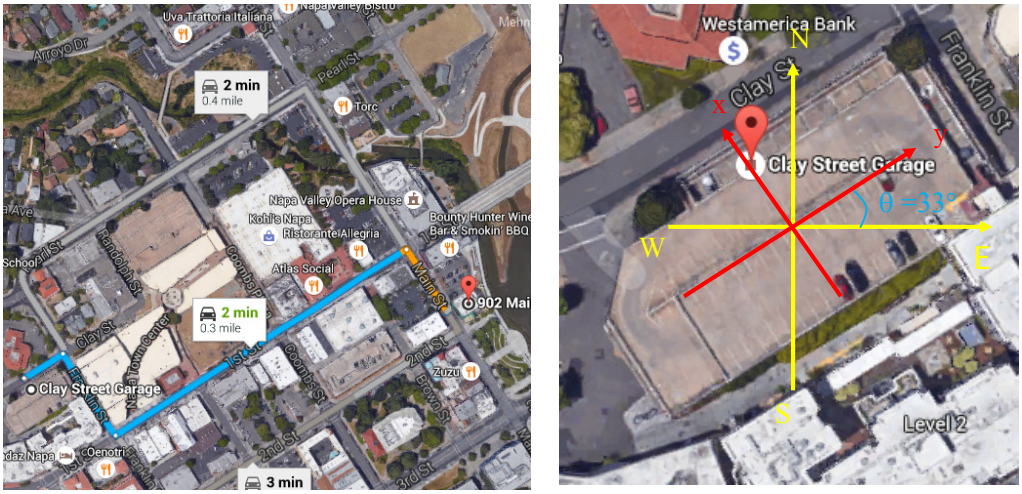

$$A_y = A_{NS}\sin\theta + A_{EW}\cos\theta$$
$$A_x = A_{NS}\cos\theta - A_{EW}\sin\theta$$

Fig. 11 – Proximity of the investigated parking structure to a ground motion recording station (left) and transformation of the recorded ground motion to the building orthogonal axes (right)

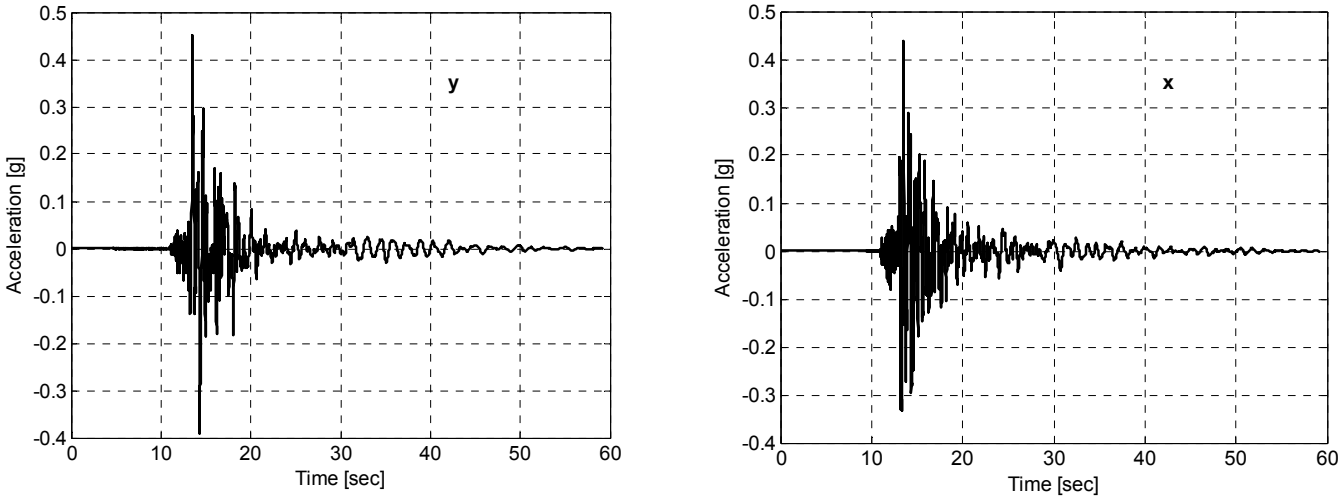

Fig. 12 – Ground accelerations along the two orthogonal directions of the investigated parking structure

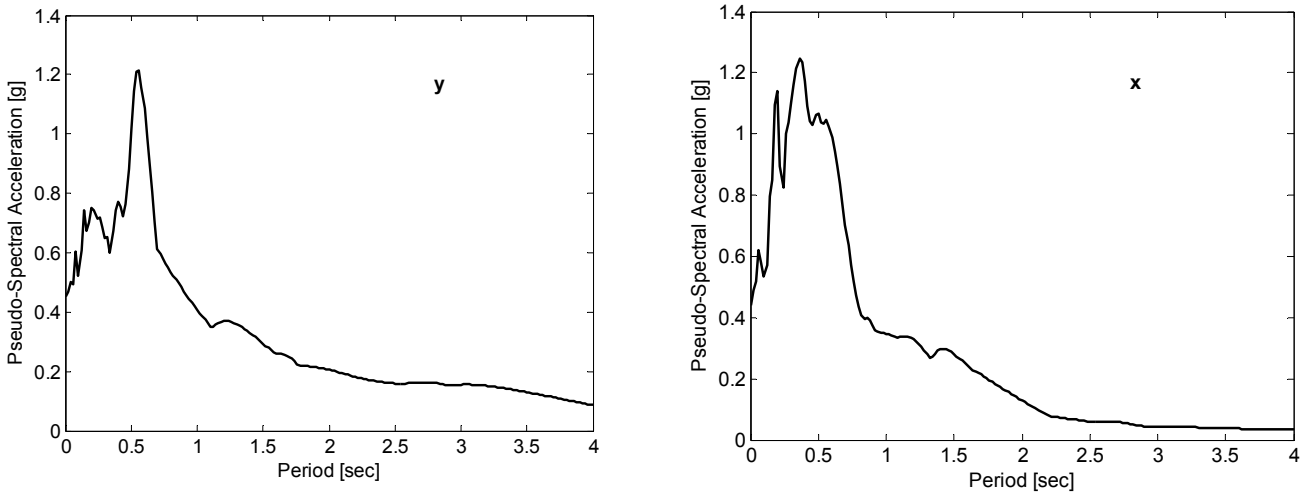

Fig. 13 – Response spectra of ground accelerations along the two orthogonal directions of the investigated parking structure

5. Piping System in the Parking Structure: Computational Model and Analysis

The main purpose of the computational modeling is to determine the structural behavior of the piping system and the interaction between the piping system and the reinforced concrete structure. Therefore, in this study, the piping system and the parking structure are jointly modeled using the finite element method (FEM). The computational model is generated using the FE software, ANSYS Workbench [6], and the geometry of the FE model of the structure is improved by the examination of the laser scanning data. In the computational model, the parking structure is modeled using SOLID65 elements. Moreover, the base of the structure is assumed to be fixed. The engineering properties used in all analyses are summarized in Table 1. A total of 687,412 elements and 1,436,246 nodes are used in the model. The detailed FE model of the piping system and the parking structure are shown in Fig. 14. Within the scope of the conducted study, linear elastic material behavior is considered for both the building and the piping system. It is noted that the weight of the water inside of the pipes was ignored.

Table 1. Mechanical properties of the construction materials

Materials	Young Modulus (MPa)	Poisson Ratio	Specific Weight (kN/m^3)
Concrete	3E+4	0.18	23.00
Steel	2E+5	0.30	78.50

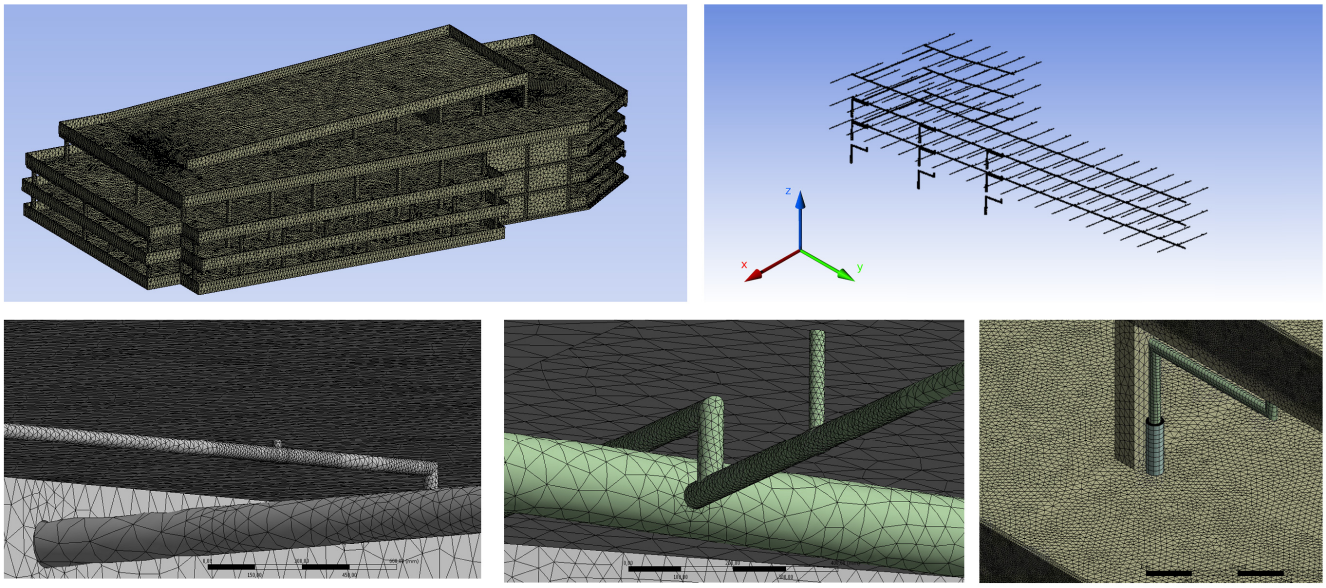

Fig 14 – Detailed finite element model of the structure and the piping system with zoomed in views

5.1. Gravity Analysis

Self-weight of the structure is an important parameter for the structural and nonstructural behavior. Therefore, static analysis due to self-weight is first performed using the computational model. The analysis indicated a maximum principal stress (tension) of 129.42 MPa, which occurred at the connection section between the hanger rots and the steel pipes and the transition zone from the steel pipes to the reinforced concrete structure (Fig. 15). Furthermore, the minimum principal stress (compression) is determined to be 114.68 MPa above the lower section of the hanger rods (Fig. 16). The maximum displacement at the center of the fourth floor slab is about 15.15 mm and the maximum displacement of the steel pipes is 13.94 mm (Fig. 17).

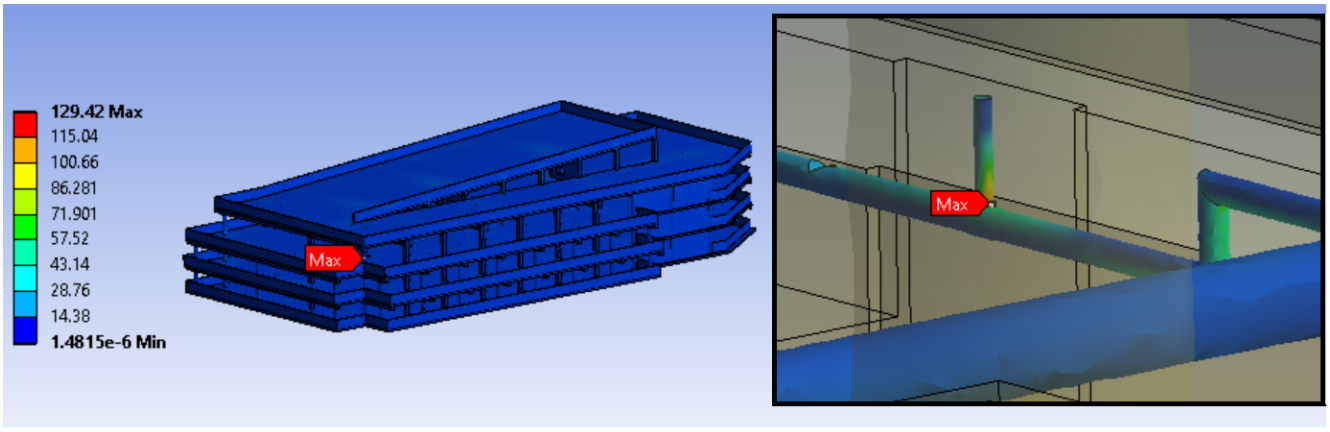

Fig 15 – Maximum principal stresses from the gravity load analysis (MPa)

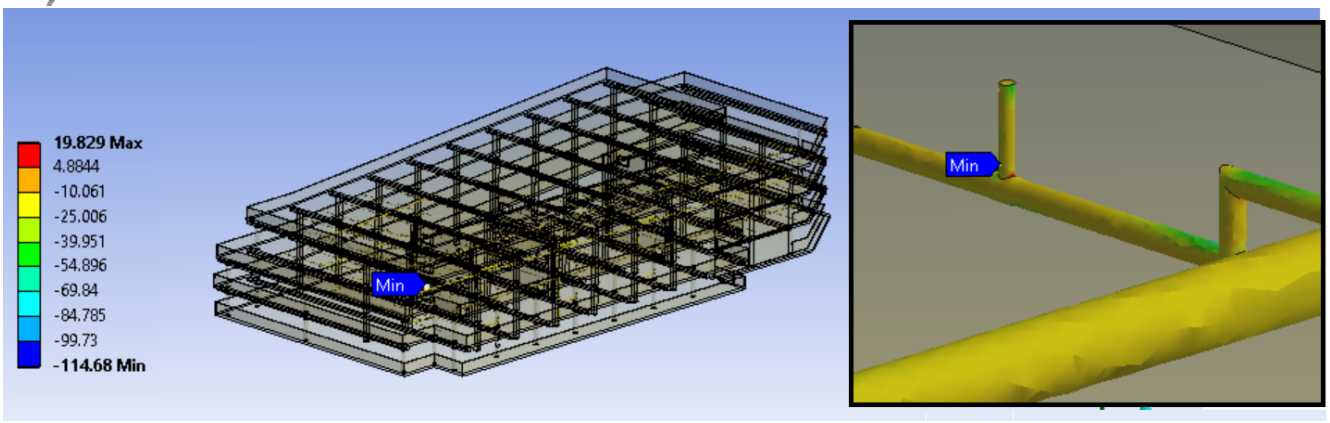

Fig. 16 – Minimum principal stresses from the gravity load analysis (MPa)

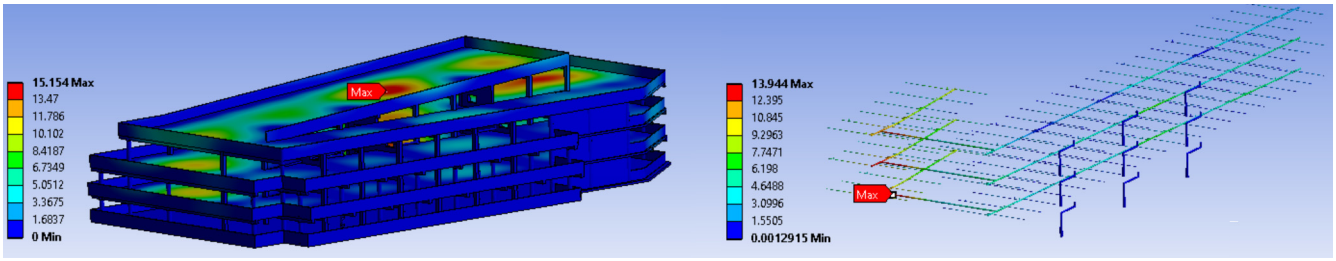

Fig. 17 – Vertical displacements from the gravity load analysis (mm)

5.2. Modal Analysis

The modal analysis is primarily used for quantifying the dynamic characteristics of the structure. The first six mode shapes are shown in Fig. 18 with the corresponding first six periods of vibration listed in Table 1. Modal analysis indicate that the torsional mode occurs in the first mode with T=0.28 sec. It is observed that modes 2 to 6 are localized at specific parts of the slabs, indicating corresponding potential dynamic response, which can affect the investigated piping systems. According to modal analysis results obtained, vertical slab vibration in Z direction is observed in modes 2-6.

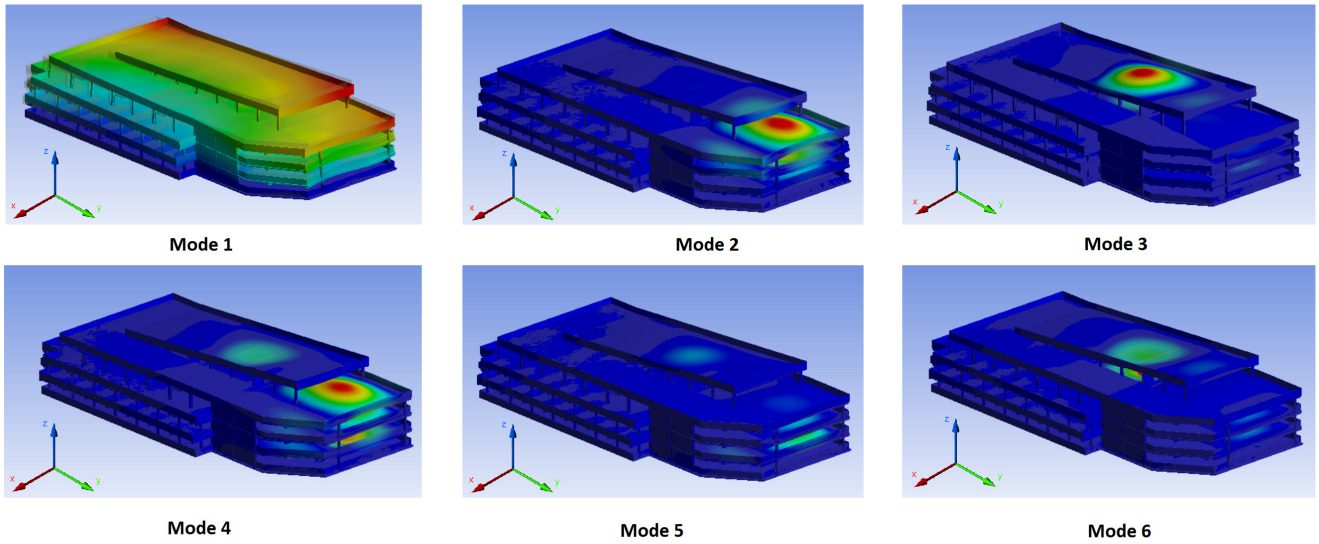

Fig. 18 – First six mode shapes of the parking structure

Table. Modal periods of the first six modes of the parking structure

Mode	1	2	3	4	5	6
Period (sec)	0.28	0.21	0.20	0.20	0.19	0.19

5.3. Time History Analysis

The time history analysis shows that the critical stresses are observed primarily at the upper section of the hanger rods. The maximum principal stresses (tension) are especially notable at the upper parts of hanger rods with a value of 218.13 MPa (Fig. 19). The minimum principal stresses (compression) are also observed at the hanger rods that carry the piping system in the ceiling section of the reinforced concrete structure with a value of 190.54 MPa (Fig. 20). The results of the analyses show that the stresses are likely to yield the steel pipes and possibly result in local or global buckling. Finally, the maximum lateral displacements take place at the top section of the structure and middle section of the piping system with a value of 16.76 mm (Fig. 21).

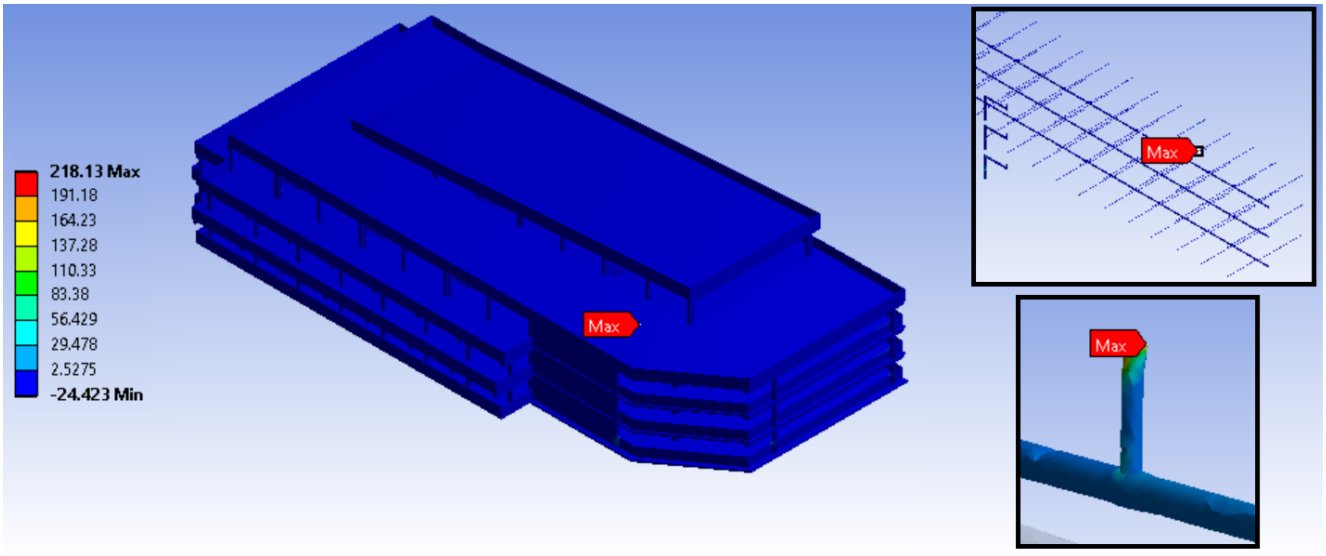

Fig. 19 – Maximum principal stresses from the time history analysis of the parking structure (MPa)

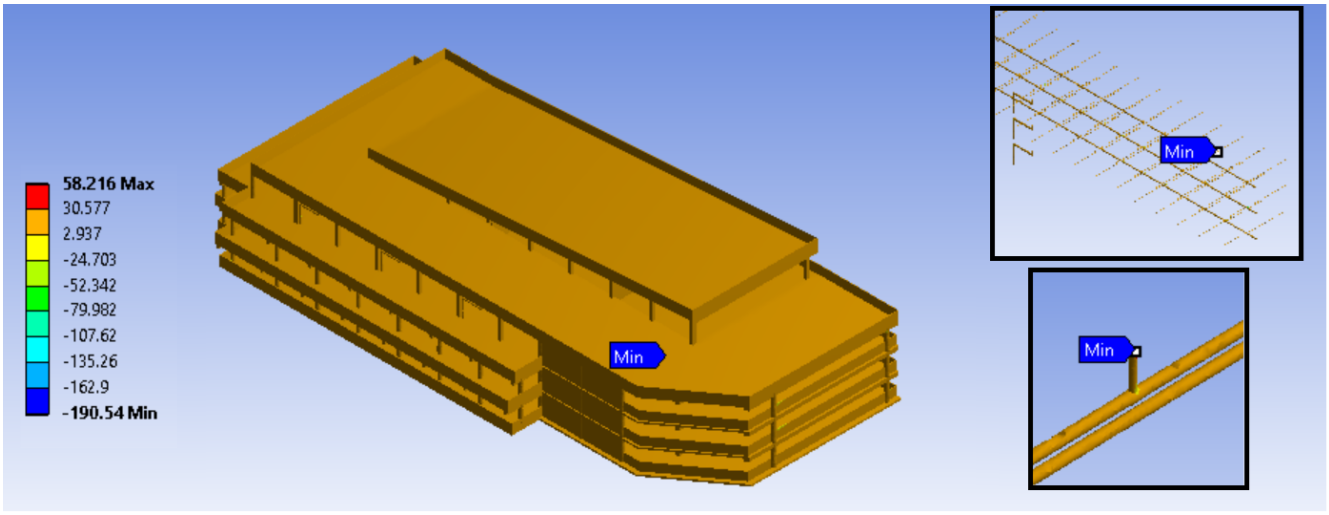

Fig. 20 – Minimum principal stresses from the time history analysis of the parking structure (MPa)

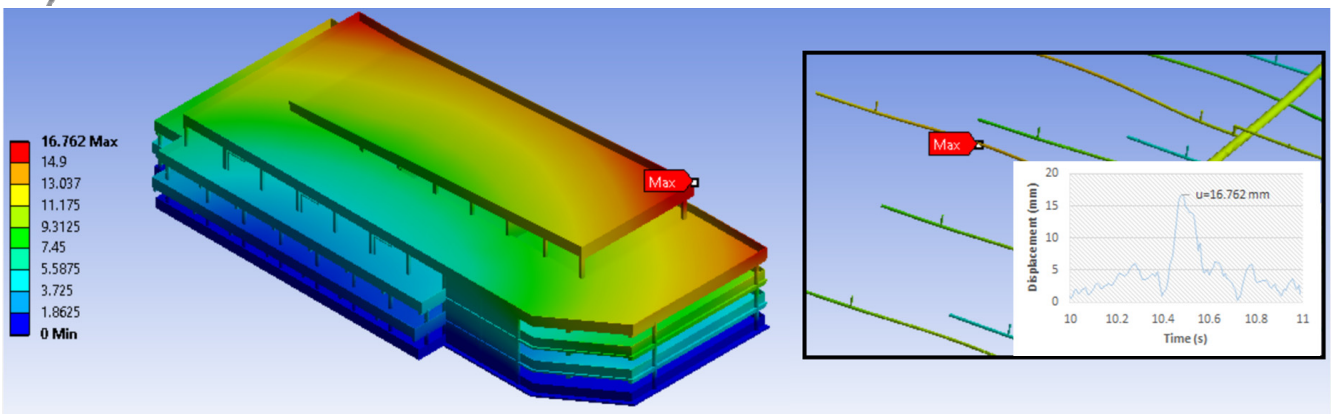

Fig. 21 – Lateral displacements from the time history analysis of the parking structure (mm)

6. Summary and Conclusions

Seismic performance of fire sprinkler systems during the 2014 South Napa earthquake were discussed and investigated in this paper. Laser scans were conducted for a parking structure with an exposed fire sprinkler system, which encountered a number of failures with some residual deformations. An accurate and detailed finite element computational model of the building and the fire sprinkler system was generated using the scanned geometry. Gravity load, modal, and linear elastic time history analyses were conducted using this model. In the time history analysis, the three components of a ground motion recorded near the building were used. The analysis results indicated the damage potential of the fire sprinkler system and were able to capture the potential of yielding and buckling of the hanging rods.

7. Acknowledgements

The laser scans were collected during operations of nees@berkeley which was supported by the National Science Foundation (NSF). Special thanks are due to Smart Scanning Solutions, LLC (Tashkent, Uzbekistan) for the extensive work on converting the point cloud into solids.

8. References

[1] FEMA, 2015. Performance of Buildings and Nonstructural Components in the 2014 South Napa Earthquake (FEMA P-1024).

[2] PEER, 2014. PEER Preliminary Notes and Observations on the August 24, 2014 South Napa Earthquake, Pacific Earthquake Engineering Research Center Report No. 2014/13, edited by G.S. Kang and S.A. Mahin, University of California, Berkeley. http://peer.berkeley.edu/publications/peer_reports/reports_2014/webPEER-2014-13-Napa.pdf.

[3] http://napavalleyregister.com, 2015. Quake-damaged McCaulou's department store won't reopen. Jul 30.

[4] http://www.statista.com, 2015. The Statistics Portal: Statistics and Studies from more than 18,000 Sources.

[5] Leica Geosystems, AG. (2015): Cyclone Version 9.1.

[6] Moaveni, S. (2003). *Finite element analysis: Theory and application with ANSYS*. Pearson Education India.

[7] MathWorks, Inc. (2015): Matlab Version 15b.